Biomedical Signal Processing and Control 68 (2021) 102736

Contents lists available at ScienceDirect

Biomedical Signal Processing and Control

journal homepage: www.elsevier.com/locate/bspc

Integral pulse frequency modulation model driven by sympathovagal dynamics: Synthetic vs. real heart rate variability

Diego Candia-Rivera [a,*], Vincenzo Catrambone [a], Riccardo Barbieri [b], Gaetano Valenza [a]

[a] Bioengineering and Robotics Research Center E. Piaggio & Department of Information Engineering, School of Engineering, University of Pisa, 56122, Pisa, Italy
[b] Department of Electronics, Informatics, and Bioengineering, Politecnico di Milano, 20133, Milano, Italy

ARTICLE INFO

Keywords:
Heart-rate variability
Integral pulse frequency modulation
Sympathovagal modulation
Sympathetic activity
Parasympathetic activity
Brain-heart interplay

ABSTRACT

Computational models that generate synthetic heart rate variability (HRV) series constitute important tools for the assessment of the effect of autonomic nervous system activity on cardiovascular control, and for the evaluation of novel algorithms using synthetic data. A widely used technique for synthetic HRV generation is the integral pulse frequency modulation (IPFM) model; however, IPFM relies on the HRV spectral paradigm, which cannot separate sympathetic and vagal oscillations that are overlapped in the low-frequency band (0.04–0.15 Hz). To overcome this limitation, a novel IPFM-inspired model driven by cardiac sympathetic and vagal dynamics estimated from HRV is proposed, where our recently developed sympathetic and parasympathetic activity indices that rely on orthonormal Laguerre expansions of the RR interval autoregressive kernels are exploited. The performance of the proposed model is evaluated by comparing the synthetic vs. real RR interval series in a simulation study involving postural changes, with real HRV data gathered from 10 healthy subjects. Moreover, the performance of the proposed model is compared with that of the standard IPFM to discern different autonomic control states associated with resting and postural changes. The results confirm that the proposed physiologically inspired model adequately predicts RR intervals during resting and postural changes. The proposed model clearly outperforms the standard IPFM method, considering both median error, and maximum error. The developed model provides valuable insights for a better understanding of the sympathovagal activity in the analysis of heartbeat dynamics.

1. Introduction

Heart rate variability (HRV) is associated with variations in the intervals between subsequent heartbeats or equivalently in the instantaneous heart rate (HR). The computational analysis of cardiac activity through HRV has been acknowledged as a standard in both research and clinical practice [1–3]. The advantages of HRV analysis is mainly attributed to its easy and non-invasive application to assess meaningful physiological and pathological correlates of several HRV markers [4–6]. HRV studies have also enabled physiological characterisation of life processes, such as emotions [7–10], attention and decision making [11], and physical exercise [12], thereby prompting the development of commercial devices to derive HRV markers [13].

Heartbeat generation has generally been described as a result of continuous interactions within the autonomous nervous system (ANS), specifically its sympathetic and parasympathetic branches [14]. Moreover, such interactions with the central nervous system (CNS) are crucial for heartbeat dynamics through the neurovisceral regulatory system activity involved in several physiological processes [15]. This interdependence is often defined as the *brain–heart interplay* [16,17].

In the context of HRV analysis, computational modelling has been employed to generate synthetic series of heartbeat dynamics, which help to understand and exploit ANS dynamics in different health and disease conditions [18]. Among the different models that have been proposed to generate phantom ECGs or HRV series, one of the popular schemes is integral pulse frequency modulation (IPFM), whose initial formulation was proposed in 1975 [19], with several variations since then [20–23].

IPFM-based models draw analogies between information transmission from the ANS and heartbeat generation, where the estimate of the controlling signal can be obtained from the latter [24]. These models are developed under the hypothesis of the existence of a *heart function* as a real-time modulation function representing stimulation of the sinoatrial node, which is directly related to heartbeat generation [25]. The advantages of the IPFM-based models for studying heartbeat dynamics

* Corresponding author.
E-mail address: d.candiarivera@studenti.unipi.it (D. Candia-Rivera).

https://doi.org/10.1016/j.bspc.2021.102736
Received 29 October 2020; Received in revised form 23 March 2021; Accepted 7 May 2021
Available online 18 May 2021

include their simplicity and real-time capacity for assessing heart modulations, particularly on the sinoatrial node, which is of interest in pathological conditions [20]. The modulation function in IPFM models considers the HRV spectral components as the inputs to an integrator that generates the heartbeats [18,20,26]. The derivation of these markers enables estimation of the sympathetic and parasympathetic activity by HRV spectral integration at low frequencies (LF: 0.04–0.15 Hz) and high frequencies (HF: 0.15–0.4 Hz), respectively [27,28]. However, it has been demonstrated that the spectral components of the ANS series generating heartbeats cannot be estimated from HRV spectral analysis. Moreover, the HRV spectral approach is susceptible to biased measurements of ANS activity given that the fixed subdivisions in defined frequency ranges (LF and HF), or their ratio, cannot successfully measure the ongoing sympathetic and parasympathetic activity fluctuations [29,30]. Some studies have suggested alternative spectral HRV analysis to better capture ANS dynamics [31,32], nevertheless, the standard spectral approach comes with limitations given that sympathetic and parasympathetic activities partly overlap in the LF frequency range [1].

More recent developments have shown that instead of analysing HRV in the spectral domain, alternative expansions of the RR series, such as the Laguerre expansion, may enable understanding cardiac dynamics better than under classical HRV analysis methods [33,34]. New indices derived from the Laguerre expansion, namely the sympathetic activity index (SAI) and parasympathetic activity index (PAI), have been reported to accurately estimate variations of the sympathovagal tone in healthy subjects [35]. These biomarkers have been proven to be accurate even in pathological conditions, particularly in patients with congestive heart failure [36], where the sympathetic nerve functions are altered [37].

In light of these promising novel sympathovagal measurements and the lack of a computational model for heartbeat dynamics to accurately account for the separate activity of the ANS branches, we propose a physiologically inspired HRV-dynamic generative model based on the standard IPFM model with SAI and PAI. We then validate the proposed model by estimating the ANS components in a group of healthy subjects under the tilt-table protocol, which is a standard for eliciting ANS effects [12,38–41]. Experimental results show that the proposed model could accurately generate physiological series under various conditions, while outperforming the original IPFM model.

2. Materials and methods

2.1. Experimental protocol

We used a publicly available dataset of postural changes in the experiments to validate the proposed method; this dataset can be downloaded from https://physionet.org/content/prcp/1.0.0/ [42,43] and comprises time series information from 10 healthy subjects (5 males and 5 females, age 28.7 ± 1.2 years on average) recorded with a one-lead ECG while undergoing the tilt-table test. The subjects were initially asked to remain in a horizontal supine position and to move to a vertical position with the help of either the tilt-table or by self-stand up. The subjects were part of six sessions that were sorted randomly between resting periods: two stand up, two slow tilt (50 s from 0 to 70°), and two fast tilt (2 s from 0 to 70°), while remaining in each condition for approximately 3 min. The entire protocol lasted between 55 and 75 min for each subject.

2.2. Estimation of sympathetic and vagal activity from heartbeat dynamics

The R-peaks from the subject ECGs were detected automatically with the Pan–Tompkins method [44], and we consecutively corrected the RR series, for misdetections or ectopic beats, using a point-process algorithm [45]. The sympathetic and parasympathetic activity were gathered from a model for sympathovagal estimation based on the Laguerre expansions, as proposed in [35]. In brief, the series of RR intervals were convolved with a set of Laguerre functions φ_j, as shown in Eq. (1), where j represents the j^{th} order Laguerre filter, and k is the k^{th} RR interval:

$$L_j(k) = \sum_{n=0}^{k-1} \varphi_j(n) \cdot RR(k - n - 1) \tag{1}$$

Therefore, the RR series can be expanded using the convolved Laguerre functions $L(k) = [L_0(k), L_1(k), \ldots, L_8(k)]^T$, and the theoretical autoregressive model can be used to separate the sympathetic and parasympathetic components as follows:

$$RR(k) = g_0(k) + \sum_{j=0}^{1} g_{1,j}(k) \cdot L_j(k) + \sum_{j=2}^{8} g_{1,j}(k) \cdot L_j(k) \tag{2}$$

The time-varying Laguerre coefficients $g(k) = [g_0(k), g_{1,0}(k), \ldots, g_{1,8}(k)]^T$ are modelled according to a dynamic system that fulfils Eqs. (3) and (4).

$$g(k) = g(k-1) + \varepsilon_g(k) \tag{3}$$

$$RR(k) = L(k)^T g(k) + \varepsilon_{RR}(k) \tag{4}$$

where ε_g is the state noise and ε_{RR} is the observation noise. The coefficients are then estimated using a Kalman filter with a time-varying observation matrix [46], and SAI and PAI are finally estimated as shown in Eqs. (5) and (6).

$$SAI(k) = \left[\Psi s_0 + \sum_{j=1}^{2} \Psi s_j \cdot g_{1,j-1}(k) \right] \Big/ RR(k) \tag{5}$$

$$PAI(k) = \left[\Psi p_0 + \sum_{j=1}^{7} \Psi p_j \cdot g_{1,j+1}(k) \right] \cdot 2RR(k) \tag{6}$$

Here, Ψs_j and Ψp_j are the generalised values for the sympathetic and parasympathetic kernels with numeric values of Ψs_j = {39.2343, 10.1963, -5.9242} and Ψp_j = {28.4875, -17.3627, 5.8798, 12.0628, 5.6408, -7.0664, -5.6779, -3.9474}. For a comprehensive description of the model generation and parametrisation, please see [35]. The SAI and PAI computation is freely available online at https://www.saipai-hrv.com.

2.3. IPFM model driven by sympathovagal dynamics

We propose a physiologically inspired model for heartbeats generation, which does not require training or parameter's fitting. Heartbeat generation models are based on the integration of a modulation function, i.e., an IPFM model. Here, we compare the use of two IPFM models: a standard approach based on the classical HRV spectral estimates, and a new approach based on SAI and PAI metrics for sympathovagal dynamics.

The IPFM models are grounded on a heartbeat generation function $x(t)$ is modelled as a sum of Dirac functions $\delta(t)$ that are activated at the instances of heartbeat occurrences t_k:

$$x(t) = \sum_{k=1}^{N} \delta(t - t_k) \tag{7}$$

The beat-to-beat generation comprises an integration within the interval from t_k to t_{k+1} on a modulation function of autonomic activity $m(t)$. When the integral function reaches a threshold (equal to 1), the heartbeat is generated, as shown in Eq. (8), where μ_{HR} corresponds to the mean HR (expressed in Hz) of the time window in which heartbeats are being modelled.

$$1 = \int_{t_k}^{t_{k+1}} [\, \mu_{HR} + m(t) \,]\, dt \tag{8}$$

The model considers that the first heartbeat occurs at $t = 0$, and the integrator over time is reset to 0 when the threshold is reached. Thus, the IPFM model generates heartbeats at fixed frequencies defined by the mean HR, and the time-varying disruptions of the HR are defined by the sympathetic and parasympathetic inputs in $m(t)$. The modulation function $m(t)$ is the model component estimated through two different approaches in this study: Standard IPFM model, and Sympathovagal modulation model.

2.3.1. Standard IPFM model

We considered the IPFM model proposed by *Brennan et al.* [26] that describes the modulation function $m(t)$ as a summation of two oscillators representing the sympathetic and parasympathetic autonomic outflows, though grounded in the HRV spectral paradigm:

$$m(t) = C_S(t) \cdot sin(\omega_s\, t) + C_P(t) \cdot sin(\omega_p\, t) \tag{9}$$

where ω_s and ω_p are the central frequencies in rad/s, and C_S and C_P are the time-varying coupling constants of the sympathetic and parasympathetic activity, respectively.

The coupling constants are defined parametrically from the Poincaré plot [26] as follows:

$$\begin{bmatrix} C_S \\ C_P \end{bmatrix} = \frac{1}{\gamma} \begin{bmatrix} \frac{sin(\omega_p / 2\mu_{HR})\, \omega_s\, \mu_{HR}}{4\, sin(\omega_s / 2\mu_{HR})} & \frac{-\sqrt{2}\, \omega_s\, \mu_{HR}}{8\, sin(\omega_s / 2\mu_{HR})} \\ \frac{-sin(\omega_s / 2\mu_{HR})\, \omega_p\, \mu_{HR}}{4\, sin(\omega_p / 2\mu_{HR})} & \frac{\sqrt{2}\, \omega_p\, \mu_{HR}}{8\, sin(\omega_p / 2\mu_{HR})} \end{bmatrix} \begin{bmatrix} L \\ W \end{bmatrix} \tag{10}$$

$$\gamma = sin(\omega_p / 2\mu_{HR}) - sin(\omega_s / 2\mu_{HR}) \tag{11}$$

where L and W are the length and width of the Poincaré plot, respectively. For the purpose of this study, the IPFM model was simulated using a 15 s long time window with an 80 % overlap to estimate the coefficients. The central frequencies used were $\omega_s = 2\pi \cdot 0.1\ rad/s$ and $\omega_p = 2\pi \cdot 0.25\ rad/s$.

2.3.2. Sympathovagal modulation model

We model the modulation function $m(t)$ as a linear combination of the sympathetic and parasympathetic activity, which can be quantified through SAI and PAI, and their respective coupling coefficients with the CNS, expressed as C_{SAI} and C_{PAI}:

$$m(t) = C_{SAI}(t) \cdot SAI(t) + C_{PAI}(t) \cdot PAI(t) \tag{12}$$

The model considers the same hypothesis for heartbeat generation as that expressed in Eqs. (7) and (8). In this model C_{SAI} and C_{PAI} are estimated using a sliding time window by a generalised linear model regression with the constant term omitted for fitting. Regression was performed using a 15 s long time window with an 80 % overlap, to estimate the coefficients. The time series were evenly sampled using spline interpolation with a 10 Hz sampling frequency, and the resulting RR series data from the model were re-centred to the original mean RR duration.

2.4. Statistical analysis

The two models of the synthetic RR series, that are, the proposed sympathovagal modulation model (SVMM) and standard IPFM model as presented in [26], were compared for the absolute percentage errors. Particularly, the model performance was evaluated using the percentage error of the generated RR series with respect to the original RR series, as shown in Eq. (13). This operation was performed for each experimental session, and the results are shown through Bland–Altman plots for all the experimental sessions.

$$Error\ \% = \left(\frac{Mean\ RR_{original} - Mean\ RR_{synthetic}}{Mean\ RR_{original}} \right) \cdot 100 \tag{13}$$

To statistically evaluate the performance of the two models in discerning resting and postural changes, we used a 2-sided non-parametric Wilcoxon signed-rank test for paired samples. The same statistical analysis was used to compare the estimated coefficients from the model as well as the SAI and PAI values. Time-varying information for all the estimated beat-to-beat features was condensed as the average value for each experimental session, and the group-wise descriptive measures are expressed as median absolute deviation (MAD).

3. Results

3.1. Model performance

We first calculated the SAI and PAI series using the RR intervals over the entire experimental session. Then, the synthetic RR series data were computed by implementing the proposed SVMM. Fig. 1 presents an example time series from a subject, specifically the original RR series and synthetic one obtained using SVMM, for both the fast tilt and preceding resting phases. As can be observed, the synthetic RR series follows the trend of the original RR dynamics.

The SVMM performance was then evaluated for all subjects after the first set of each experimental session (i.e., rest, stand up, slow tilt, and fast tilt). Fig. 2 shows the performance of the proposed model in a Bland–Altman plot, where the X-axis presents the grand averages of the RR intervals for the original and synthetic data in a specific experimental session. The Y-axis represents the percentage error of the synthetic RR interval with respect to the original. The synthetic series has a grand average error of -0.97 % compared to the original RR series, with a median of -0.89 %; this means that the synthetic RR intervals are on average less than 1% shorter than the original ones. It can also be observed that the results associated with the four different experimental

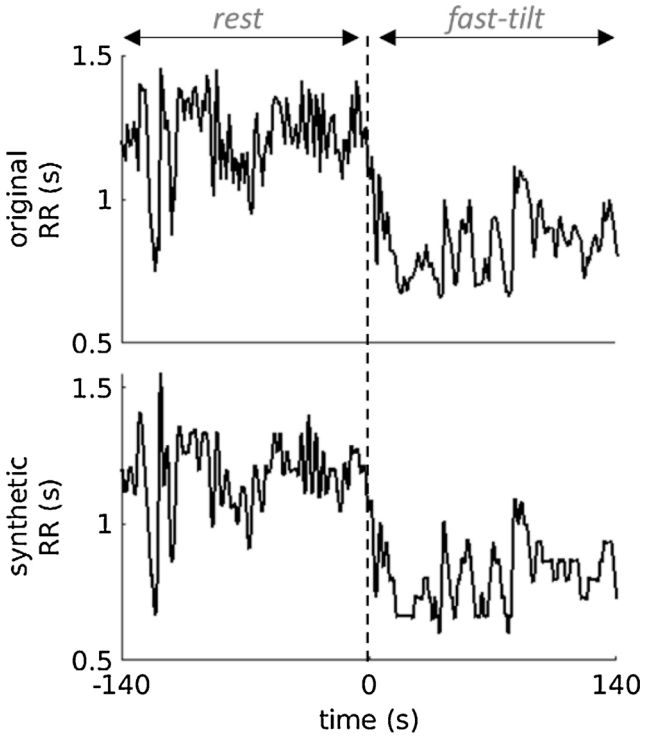

Fig. 1. RR series for one subject during change from rest to fast tilt: original RR series (top) and synthetic RR series (bottom).

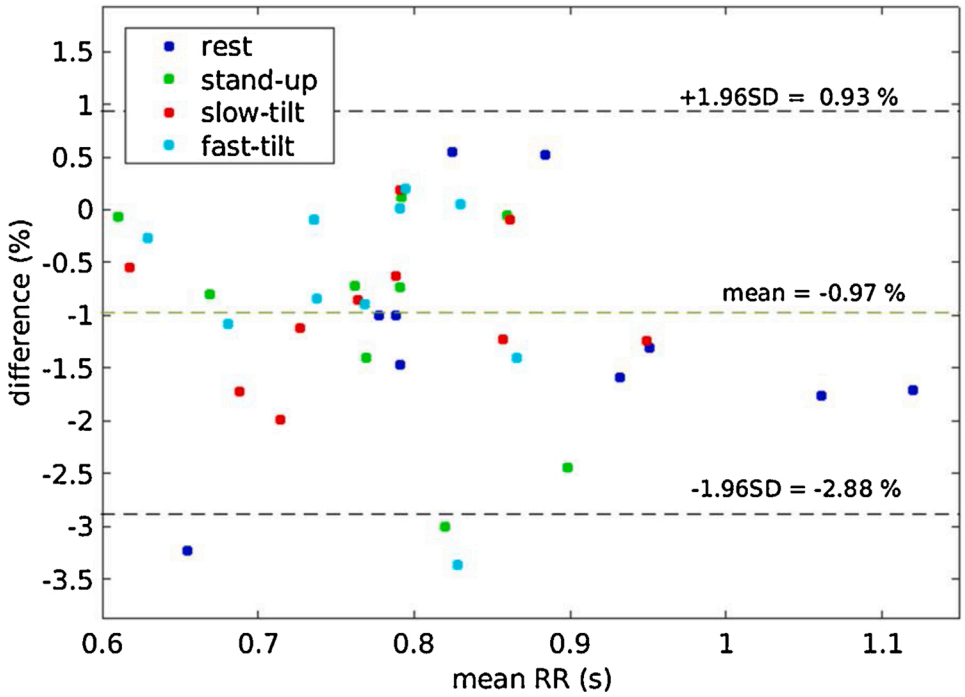

Fig. 2. Bland–Altman plot of the percentage error between real and SVMM synthetic RR measurements.

sessions do not differ in terms of dispersions in the Bland–Altman plot.

Table 1 reports the group-wise median values for the three experimental sessions for the original and synthetic RR values. It should be noted that to better appreciate the changes in the RR interval durations in the various experimental sessions, we also represent the median values associated with the preceding resting phases. Table 1 indicates that all postural changes cause significant decreases in the mean RR durations and consequently increases in the heart rates.

The p-values obtained via statistical analyses (i.e., Wilcoxon non-parametric test for paired samples) are in the range of 0.002–0.0039. Choosing an overall significance of $\alpha' = 0.05$ and applying the Bonferroni correction for six multiple comparisons, we obtained the significance threshold at $\alpha = \alpha'/6 = 0.0083$. Thus, all the postural changes, both for the analysed synthetic SVMM and original RR series data are statistically significant with respect to their preceding resting phases; specifically, postural changes were shown to shorten the RR intervals. A stronger effect, followed by a lower p-value, is obtained when the postural change is performed with the assistance of the tilt-table, both for slow and fast variations, compared to the active stand up phase.

3.2. Comparison with standard IPFM model

We compared the performance of the synthetic RR series obtained with the SVMM against the classical IPFM model [26]. In Table 2, the group-wise percentage errors for the SVMM and parametric IPFM model are reported. The performance of the RR series can be observed as percentage errors of the original data for the two models, which remain below 6.31 % under all experimental conditions. The relative error range for the IPFM model is 0.04–6.31 %, which is wider than the 0.02–3.37 % range of the SVMM.

Table 2
Absolute percentage errors with respect to the original RR series for the SVMM and IPFM model.

		SVMM (%)	IPFM (%)
Absolute error Overall range		0.02–3.37	0.04–6.31
Absolute error Median ± MAD	Overall error	0.89 ± 0.57	1.09 ± 0.52
	Rest	1.39 ± 0.38	1.25 ± 0.40
	Stand up	0.74 ± 0.66	1.03 ± 0.76
	Slow tilt	0.99 ± 0.39	0.92 ± 0.57
	Fast tilt	0.55 ± 0.48	1.02 ± 0.55

3.3. Sympathovagal components analysis

Both the models compared here rely on the estimation of parameters quantifying the sympathetic and parasympathetic time-varying activity. The time courses of these parameters are remarkably altered by the postural changes of the subjects.

Fig. 3 presents an example time series from a subject, where the grey areas represent posture change phases and white areas represent resting phases. The five panels of the figure present the time courses of the original RR series, SAI, PAI, C_{SAI}, and C_{PAI} separately. Fig. 3 shows a clear decrease in the RR interval when a posture change is noted; this change is derived from a simultaneous increase in the sympathetic activity, measured with the SAI, and decrease in parasympathetic activity,

Table 1
Mean of the RR intervals under the three types of postural changes, and p-values from statistical comparisons between the posture changes and preceding resting phases.

	Original RR (s)			SVMM synthetic RR (s)		
	Rest	Posture change	p	Rest	Posture change	p
Stand up	0.86 ± 0.09	0.78 ± 0.06	0.0039	0.87 ± 0.08	0.78 ± 0.06	0.0039
Slow tilt	0.87 ± 0.08	0.78 ± 0.07	0.0020	0.87 ± 0.08	0.77 ± 0.07	0.0020
Fast tilt	0.85 ± 0.08	0.78 ± 0.05	0.0020	0.85 ± 0.08	0.78 ± 0.04	0.0020

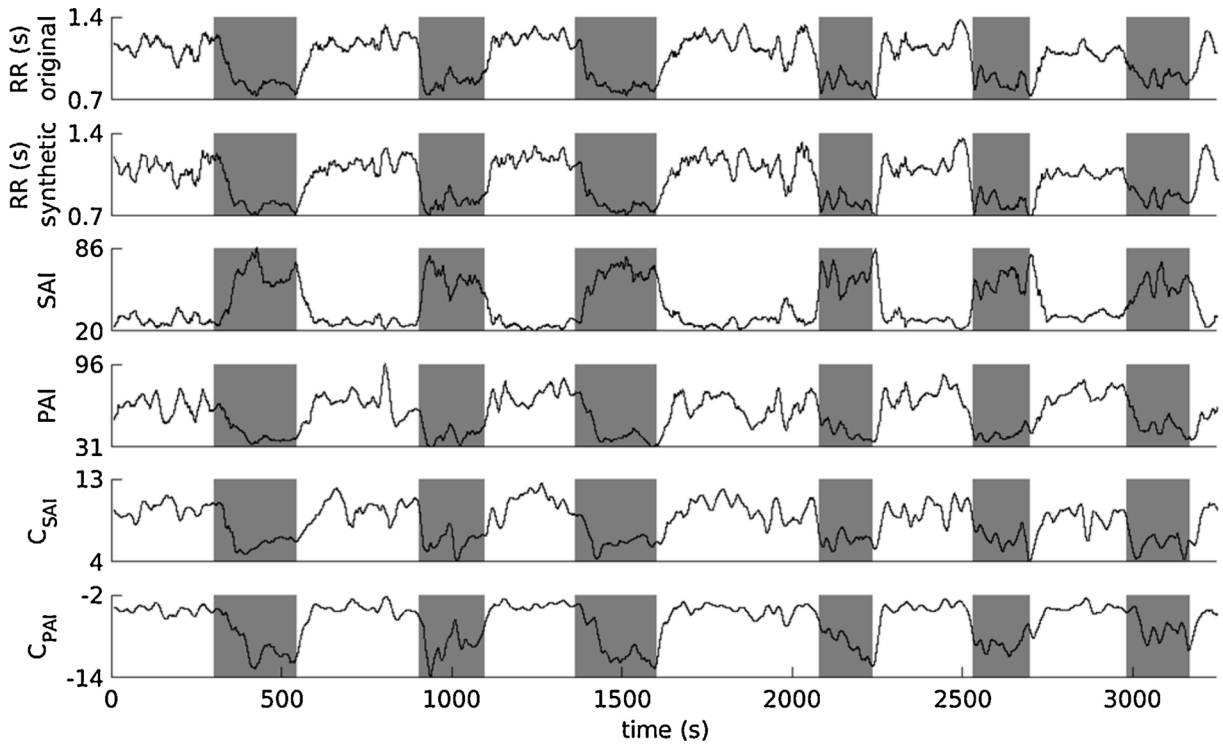

Fig. 3. Example changes in the HRV markers of one subject. The shaded areas correspond to posture changes. All measurements are in arbitrary units except where explicitly indicated.

measured with the PAI. Both C_{SAI} and C_{PAI} show decreases for all posture change phases during shorter RR intervals.

Tables 3 and 4 summarise the group-wise averages of the coefficients quantifying ANS branch activity, that is, SAI, PAI, C_{SAI}, C_{PAI}, (results related to SAI and PAI are in Table 3, and those related to C_{SAI} and C_{PAI} are in Table 4). The variations induced by postural changes with respect to the preceding resting phase can be observed both in terms of absolute values and statistical comparisons via the Wilcoxon signed-rank test. The changes from rest to tilt, both slow and fast, are always statistically significant (i.e., p-values < 0.0083); only the C_{SAI} index has a p-value greater than 0.002. Conversely, group-wise changes from rest to stand up do not show significant variations in the computed model components.

4. Discussion

In this study, we propose a physiologically inspired SVMM for HRV that is able to generate realistic synthetic data. The proposed model considers the cardiac sympathetic and parasympathetic activity as inputs, quantified through SAI and PAI series, to generate synthetic RR series as the output, and it was developed on the basis of the standard IPFM model. We validated the proposed model on a publicly available HRV dataset with information from 10 subjects who underwent postural changes from horizontal to upright positions during the experiments [43]. The synthetic HRV series were generated using the proposed model with high consistency and real RR intervals for all the experimental conditions. Results showed that the synthetic data closely reproduced the trends of the original RR series with low error (overall median error < 0.9 %). Only three points surpassed the Bland-Altman plot lower limit; as these points were related to different experimental phases (rest, stand-up and fast tilt), the SVMM model's performance does not change as a function of the experimental conditions. The results from the SVMM were consistent with those reported in the literature and showed significant decreases in the RR intervals during postural changes [12,38–41]; these results were also confirmed by comparisons with synthetic RR series generated with the IPFM model (see Fig. 1 and Table 1).

We compared the synthetic series generated using the proposed model with those obtained from the standard parametric IPFM model proposed by *Brennan et al.* [26]. The results show that the SVMM performance is comparable to that of the IPFM model, showing low percentage errors under all experimental conditions; this indicates that the SVMM is a suitable alternative for physiological modelling of cardiac dynamics. Notably, the proposed SVMM is non-parametric, which is advantageous because fewer assumptions are required; moreover, it is inspired by other physiological processes comprising reliable and separate estimations of the sympathetic and vagal components [35]. The IPFM model used as a comparison depends on two parameters that are based on the geometry of the Poincaré plot, which may cause higher sensitivities to errors and artefacts [47]. The promising applicability of the proposed non-parametric method for synthetic RR series generation thus relies on the robustness of the model, which remains to be tested

Table 3
SAI and PAI computed for the three types of postural changes, and p-values from statistical comparisons between postural changes and their preceding resting phases.

	SAI			PAI		
	Rest	Posture change	p-value	Rest	Posture change	p-value
Stand up	50.61 ± 14.79	69.22 ± 5.80	0.1641	51.04 ± 7.63	42.99 ± 3.08	0.4961
Slow tilt	56.40 ± 11.25	73.23 ± 13.01	0.0020	54.24 ± 7.03	43.84 ± 3.77	0.0020
Fast tilt	58.24 ± 13.10	72.71 ± 10.04	0.0020	50.73 ± 4.47	43.60 ± 3.92	0.0020

Table 4
C_{SAI} and C_{PAI} computed for the three types of postural changes, and p-values from statistical comparisons between postural changes and their preceding resting phases.

	C_{SAI}			C_{PAI}		
	Rest	Posture change	p-value	Rest	Posture change	p-value
Stand up	6.91 ± 1.16	5.73 ± 0.09	0.3594	−7.09 ± 1.48	−8.65 ± 1.01	0.2500
Slow tilt	6.36 ± 0.75	5.57 ± 0.21	0.0039	−6.90 ± 1.19	−8.80 ± 0.86	0.0020
Fast tilt	6.16 ± 0.66	5.67 ± 0.47	0.0098	−7.22 ± 1.05	−9.26 ± 0.75	0.0020

under different experimental conditions.

A limitation of this study is related to the restricted number of real HRV recordings on which the proposed model has been tested; however, it should be noted that our aim was to evaluate a new IPFM-based computational model that overcomes some limitations associated with the HRV spectral paradigm, and applications of this new modeling framework are part of our future endeavors.

From a physiological point of view, the proposed model addresses the known problems of sympathetic and parasympathetic activity estimations from HRV [1,28–31,48]. Accordingly, the SVMM utilises the SAI and PAI markers, which have demonstrated more efficient capabilities for disentangling the sympathetic and parasympathetic activity compared to classical HRV spectral measures [35]. The proposed SVMM comprises a linear combination of the SAI and PAI. We evaluated these markers for their abilities to discriminate the variations between rest and postural changes, with significant results for slow and fast tilts, as expected from reported literature [12,38–41]. The coupling coefficients of the IPFM model have been shown to help uncover modulations between the brain and heart dynamics [49]. Hence, enhanced modelling of cardiac dynamics may pave the way for further developments on understanding the ANS and brain–heart interplay for specific components, directionalities, and latencies [16,49].

5. Conclusion

The physiological modelling of bodily signals can help determine the underlying aspects of ANS dynamics for cardiovascular control in terms of the time-varying modulations of specific components that are of particular interest in pathological conditions [20]. The results presented herein indicate that synthetic data generation based on sympathovagal activity quantified through the SAI and PAI [35] may correspond with those for realistic HRV series, and this might enable the development of computational simulations aimed at a better understanding of the cardiovascular and physiological system dynamics. The proposed model can be considered as a new tool for the analysis of HRV that allows physiologically inspired computational modelling, which can help a better understanding of the sympathovagal balance dynamics in the future.

Funding

The research leading to these results has received partial funding from the European Commission - Horizon 2020 Program under grant agreement n° 813234 of the project “RHUMBO”, and from the Italian Ministry of Education and Research (MIUR) in the framework of the CrossLab project (Departments of Excellence).

CRediT authorship contribution statement

Individual authors’ contributions are: **Diego Candia-Rivera, Riccardo Barbieri and Gaetano Valenza:** designed the study. **Diego Candia-Rivera, Riccardo Barbieri, and Gaetano Valenza:** processed the data. **Diego Candia-Rivera, Vincenzo Catrambone and Gaetano Valenza:** analyzed the data. **Diego Candia-Rivera, Vincenzo Catrambone, Riccardo Barbieri and Gaetano Valenza:** wrote and reviewed the paper.

Declaration of Competing Interest

The authors declare that they have no known competing financial interests or personal relationships that could have appeared to influence the work reported in this paper.

References

[1] Task Force of the European Society of Cardiology the North American Society of Pacing, Heart rate variability: standards of measurement, physiological interpretation, and clinical use, Circulation 93 (1996) 1043–1065, https://doi.org/10.1161/01.CIR.93.5.1043.
[2] U. Rajendra Acharya, K. Paul Joseph, N. Kannathal, C.M. Lim, J.S. Suri, Heart rate variability: a review, Med. Biol. Eng. Comput. 44 (2006) 1031–1051, https://doi.org/10.1007/s11517-006-0119-0.
[3] F. Shaffer, R. McCraty, C.L. Zerr, A healthy heart is not a metronome: an integrative review of the heart’s anatomy and heart rate variability, Front. Psychol. 5 (2014), https://doi.org/10.3389/fpsyg.2014.01040.
[4] M. Böhm, K. Swedberg, M. Komajda, J.S. Borer, I. Ford, A. Dubost-Brama, G. Lerebours, L. Tavazzi, Heart rate as a risk factor in chronic heart failure (SHIFT): the association between heart rate and outcomes in a randomised placebo-controlled trial, Lancet 376 (2010) 886–894, https://doi.org/10.1016/S0140-6736(10)61259-7.
[5] J.F. Thayer, F. Ahs, M. Fredrikson, J.J. Sollers, T.D. Wager, A meta-analysis of heart rate variability and neuroimaging studies: implications for heart rate variability as a marker of stress and health, Neurosci. Biobehav. Rev. 36 (2012) 747–756, https://doi.org/10.1016/j.neubiorev.2011.11.009.
[6] A.H. Kemp, D.S. Quintana, The relationship between mental and physical health: insights from the study of heart rate variability, Int. J. Psychophysiol. 89 (2013) 288–296, https://doi.org/10.1016/j.ijpsycho.2013.06.018.
[7] R. McCraty, M. Atkinson, W.A. Tiller, G. Rein, A.D. Watkins, The effects of emotions on short-term power spectrum analysis of heart rate variability, Am. J. Cardiol. 76 (1995) 1089–1093, https://doi.org/10.1016/S0002-9149(99)80309-9.
[8] M. Mather, J. Thayer, How heart rate variability affects emotion regulation brain networks, Curr. Opin. Behav. Sci. 19 (2018) 98–104, https://doi.org/10.1016/j.cobeha.2017.12.017.
[9] R.D. Lane, K. McRae, E.M. Reiman, K. Chen, G.L. Ahern, J.F. Thayer, Neural correlates of heart rate variability during emotion, Neuroimage 44 (2009) 213–222, https://doi.org/10.1016/j.neuroimage.2008.07.056.
[10] B.M. Appelhans, L.J. Luecken, Heart rate variability as an index of regulated emotional responding, Rev. Gen. Psychol. 10 (2006) 229–240, https://doi.org/10.1037/1089-2680.10.3.229.
[11] E. Ramírez, A.R. Ortega, G.A. Reyes Del Paso, Anxiety, attention, and decision making: the moderating role of heart rate variability, Int. J. Psychophysiol. 98 (2015) 490–496, https://doi.org/10.1016/j.ijpsycho.2015.10.007.
[12] N. Montano, T.G. Ruscone, A. Porta, F. Lombardi, M. Pagani, A. Malliani, Power spectrum analysis of heart rate variability to assess the changes in sympathovagal balance during graded orthostatic tilt, Circulation 90 (1994) 1826–1831, https://doi.org/10.1161/01.cir.90.4.1826.
[13] Z. Yang, Q. Zhou, L. Lei, K. Zheng, W. Xiang, An IoT-cloud based wearable ECG monitoring system for smart healthcare, J. Med. Syst. 40 (2016) 286, https://doi.org/10.1007/s10916-016-0644-9.
[14] M. Sinski, J. Lewandowski, P. Abramczyk, K. Narkiewicz, Z. Gaciong, Why study sympathetic nervous system? J. Physiol. Pharmacol. 57 (Suppl 11) (2006) 79–92.
[15] J.F. Thayer, E. Sternberg, Beyond heart rate variability, Ann. N. Y. Acad. Sci. 1088 (2006) 361–372, https://doi.org/10.1196/annals.1366.014.
[16] G. Valenza, N. Toschi, R. Barbieri, Uncovering brain–heart information through advanced signal and image processing, Philos. Trans. R. Soc. A Math. Phys. Eng. Sci. 374 (2016), 20160020, https://doi.org/10.1098/rsta.2016.0020.
[17] D. Azzalini, I. Rebollo, C. Tallon-Baudry, Visceral signals shape brain dynamics and cognition, Trends Cogn. Sci. 23 (2019) 488–509, https://doi.org/10.1016/j.tics.2019.03.007.
[18] P.E. McSharry, G.D. Clifford, L. Tarassenko, L.A. Smith, A dynamical model for generating synthetic electrocardiogram signals, IEEE Trans. Biomed. Eng. 50 (2003) 289–294, https://doi.org/10.1109/TBME.2003.808805.
[19] B.W. Hyndman, R.K. Mohn, A model of the cardiac pacemaker and its use in decoding the information content of cardiac intervals, Automedica 1 (1975) 239–252.
[20] R. Bailón, G. Laouini, C. Grao, M. Orini, P. Laguna, O. Meste, The integral pulse frequency modulation model with time-varying threshold: application to heart rate variability analysis during exercise stress testing, IEEE Trans. Biomed. Eng. 58 (2011) 642–652, https://doi.org/10.1109/TBME.2010.2095011.

[21] J.D. Scheff, P.D. Mavroudis, S.E. Calvano, S.F. Lowry, I.P. Androulakis, Modeling autonomic regulation of cardiac function and heart rate variability in human endotoxemia, Physiol. Genomics 43 (2011) 951–964, https://doi.org/10.1152/physiolgenomics.00040.2011.
[22] D.C. McLernon, N.J. Dabanloo, A. Ayatollahi, V.J. Majd, H. Zhang, A new nonlinear model for generating RR tachograms, Comput. Cardiol. 2004 (2004) 481–484, https://doi.org/10.1109/CIC.2004.1442979.
[23] H.-W. Chiu, T.-H. Wang, L.-C. Huang, H.-W. Tso, T. Kao, The influence of mean heart rate on measures of heart rate variability as markers of autonomic function: a model study, Med. Eng. Phys. 25 (2003) 475–481, https://doi.org/10.1016/s1350-4533(03)00019-5.
[24] R.K. Mohn, Modelling the natural pacemaker of the heart as a pulse-frequency modulator, Med. Biol. Eng. Comput. 16 (1978) 90–97, https://doi.org/10.1007/BF02442939.
[25] M.N. Levy, P.J. Martin, Neural regulation of the heart beat, Annu. Rev. Physiol. 43 (1981) 443–453, https://doi.org/10.1146/annurev.ph.43.030181.002303.
[26] M. Brennan, M. Palaniswami, P. Kamen, Poincaré plot interpretation using a physiological model of HRV based on a network of oscillators, Am. J. Physiol. Heart Circ. Physiol. 283 (2002) H1873–1886, https://doi.org/10.1152/ajpheart.00405.2000.
[27] B. Pomeranz, R.J. Macaulay, M.A. Caudill, I. Kutz, D. Adam, D. Gordon, K. M. Kilborn, A.C. Barger, D.C. Shannon, R.J. Cohen, Assessment of autonomic function in humans by heart rate spectral analysis, Am. J. Physiol. 248 (1985) H151–153, https://doi.org/10.1152/ajpheart.1985.248.1.H151.
[28] G.A. Reyes del Paso, W. Langewitz, L.J.M. Mulder, A. van Roon, S. Duschek, The utility of low frequency heart rate variability as an index of sympathetic cardiac tone: a review with emphasis on a reanalysis of previous studies, Psychophysiology 50 (2013) 477–487, https://doi.org/10.1111/psyp.12027.
[29] D.S. Goldstein, O. Bentho, M.-Y. Park, Y. Sharabi, Low-frequency power of heart rate variability is not a measure of cardiac sympathetic tone but may be a measure of modulation of cardiac autonomic outflows by baroreflexes, Exp. Physiol. 96 (2011) 1255–1261, https://doi.org/10.1113/expphysiol.2010.056259.
[30] G.E. Billman, The LF/HF ratio does not accurately measure cardiac sympatho-vagal balance, Front. Physiol. 4 (2013), https://doi.org/10.3389/fphys.2013.00026.
[31] W. von Rosenberg, T. Chanwimalueang, T. Adjei, U. Jaffer, V. Goverdovsky, D. P. Mandic, Resolving ambiguities in the LF/HF ratio: LF-HF scatter plots for the categorization of mental and physical stress from HRV, Front. Physiol. 8 (2017), https://doi.org/10.3389/fphys.2017.00360.
[32] D. Candia-Rivera, J. Annen, O. Gosseries, C. Martial, A. Thibaut, S. Laureys, C. Tallon-Baudry, Neural responses to heartbeats detect residual signs of consciousness during resting state in post-comatose patients, J. Neurosci. (2021), https://doi.org/10.1523/JNEUROSCI.1740-20.2021.
[33] V.Z. Marmarelis, Identification of nonlinear biological systems using Laguerre expansions of kernels, Ann. Biomed. Eng. 21 (1993) 573–589, https://doi.org/10.1007/BF02368639.
[34] G. Valenza, L. Citi, E.P. Scilingo, R. Barbieri, Point-process nonlinear models with Laguerre and Volterra expansions: instantaneous assessment of heartbeat dynamics, IEEE Trans. Signal Process. 61 (2013) 2914–2926, https://doi.org/10.1109/TSP.2013.2253775.
[35] G. Valenza, L. Citi, J.P. Saul, R. Barbieri, Measures of sympathetic and parasympathetic autonomic outflow from heartbeat dynamics, J. Appl. Physiol. 125 (2018) 19–39, https://doi.org/10.1152/japplphysiol.00842.2017.
[36] G. Valenza, L. Citi, J.P. Saul, R. Barbieri, ECG-derived sympathetic and parasympathetic nervous system dynamics: a congestive heart failure study, 2018 Computing in Cardiology Conference (CinC) (2018) 1–4, https://doi.org/10.22489/CinC.2018.282.
[37] Eisenhofer Graeme, Friberg Peter, Rundqvist Bengt, A. Quyyumi Arshed, Lambert Gavin, M. Kaye David, J. Kopin Irwin, S. Goldstein David, D. Esler Murray, Cardiac sympathetic nerve function in congestive heart failure, Circulation 93 (1996) 1667–1676, https://doi.org/10.1161/01.CIR.93.9.1667.
[38] W.H. Cooke, J.B. Hoag, A.A. Crossman, T.A. Kuusela, K.U. Tahvanainen, D. L. Eckberg, Human responses to upright tilt: a window on central autonomic integration, J. Physiol. 517 (Pt 2) (1999) 617–628, https://doi.org/10.1111/j.1469-7793.1999.0617t.x.
[39] A. Porta, E. Tobaldini, S. Guzzetti, R. Furlan, N. Montano, T. Gnecchi-Ruscone, Assessment of cardiac autonomic modulation during graded head-up tilt by symbolic analysis of heart rate variability, Am. J. Physiol. Heart Circ. Physiol. 293 (2007) H702–708, https://doi.org/10.1152/ajpheart.00006.2007.
[40] M. Bootsma, C.A. Swenne, H.H. Van Bolhuis, P.C. Chang, V.M. Cats, A.V. Bruschke, Heart rate and heart rate variability as indexes of sympathovagal balance, Am. J. Physiol. 266 (1994) H1565–1571, https://doi.org/10.1152/ajpheart.1994.266.4.H1565.
[41] L. Bondar Roberta, T. Dunphy Paul, Peyman Moradshahi, S. Kassam Mahmood, P. Blaber Andrew, Flo Stein, R. Freeman, Cerebrovascular and cardiovascular responses to graded tilt in patients with autonomic failure, Stroke 28 (1997) 1677–1685, https://doi.org/10.1161/01.STR.28.9.1677.
[42] A.L. Goldberger, L.A. Amaral, L. Glass, J.M. Hausdorff, P.C. Ivanov, R.G. Mark, J. E. Mietus, G.B. Moody, C.K. Peng, H.E. Stanley, PhysioBank, PhysioToolkit, and PhysioNet: components of a new research resource for complex physiologic signals, Circulation 101 (2000) E215–220, https://doi.org/10.1161/01.cir.101.23.e215.
[43] T. Heldt, M.B. Oefinger, M. Hoshiyama, R.G. Mark, Circulatory response to passive and active changes in posture, Comput. Cardiol. 2003 (2003) 263–266, https://doi.org/10.1109/CIC.2003.1291141.
[44] J. Pan, W.J. Tompkins, A real-time QRS detection algorithm, IEEE Trans. Biomed. Eng. BME-32 (1985) 230–236, https://doi.org/10.1109/TBME.1985.325532.
[45] L. Citi, E.N. Brown, R. Barbieri, A real-time automated point process method for detection and correction of erroneous and ectopic heartbeats, IEEE Trans. Biomed. Eng. 59 (2012) 2828–2837, https://doi.org/10.1109/TBME.2012.2211356.
[46] G. Valenza, L. Citi, V.B. Wyller, R. Barbieri, ECG-derived sympathetic and parasympathetic activity in the healthy: an early Lower-body negative pressure study using adaptive Kalman prediction, 2018 40th Annual International Conference of the IEEE Engineering in Medicine and Biology Society (EMBC) (2018) 5628–5631, https://doi.org/10.1109/EMBC.2018.8513512.
[47] B. Singh, D. Singh, Ectopic beats and editing methods for Poincaré-plot-based HRV, Int. J. Biomed. Eng. Technol. 7 (2011) 353–364, https://doi.org/10.1504/IJBET.2011.044414.
[48] R.W. de Boer, J.M. Karemaker, J. Strackee, Spectrum of a series of point events, generated by the integral pulse frequency modulation model, Med. Biol. Eng. Comput. 23 (1985) 138–142, https://doi.org/10.1007/BF02456750.
[49] V. Catrambone, A. Greco, N. Vanello, E.P. Scilingo, G. Valenza, Time-resolved directional brain-heart interplay measurement through synthetic data generation models, Ann. Biomed. Eng. 47 (2019) 1479–1489, https://doi.org/10.1007/s10439-019-02251-y.